A Statistical Study of CME Plasma F1ows

R. Goldstein, M. Neugebauer, and D. Clay

Jet Propulsion Laboratory, California Institute of Technology, Pasadena,CA91109

Abstract. Many studies of the interplanetary manifestations of coronal mass ejections (CMEs) have focused on the shock driver gas or on the regions that display a flux-rope magnetic topology. Somewhat less attention has been paid to investigating how the solar wind returns to its ambient, pre-CME condition, A CME observed by ISEE-3 and other spacecraft during the period September 29- October 3, 1978 exhibited some interesting features which are described. Many of the plasma parameters typically associated with CME flow, such as low temperature, low beta, and high helium abundance began hours before and extended for several days after the magnetic cloud geometry and the bi-directional streaming of suprathermal electrons and energetic protons. A superposed epoch analysis of the entire ISEE-3 data set available for the 1978 to 1980 interval shows that these properties are characteristic of many of the CME flows in this period.

Introduction

Coronal Mass Ejections (CMEs) are one of the consequences of the dynamic nature of the Sun. These eruptions have been studied by many researchers both by remote sensing of the events as they occur at the sun, as well as by in situ measurements of the plasma properties using instrumentation onboard spacecraft. Although we have learned a considerable amount about the characteristics of CMES from these studies we still don't understand the basic processes involved in their origin and evolution, In fact, although a variety of signatures has been used by various authors to identify CMES during in situ measurements, there are no universally accepted criteria for defining a CME, so one author's "list" of events usually won't coincide with another's. These signatures include high helium abundance [*Hirshberg et al.,* 1972; *Borrini et al., 1982],* low ion temperatures *[Gosling et al., 1973],* hi-directional streaming (BDS) of suprathermal electrons *[Montgomery et al., 1974; Bame et al., 1981; Gosling et al., 1987; Pilipp et al., 1987]* and/or energetic ions *[Palmer et al., 1978; Kutchko et al., 1982; Sarris and Krimigis, 1982; Sanderson et al.,* 1983; *Pilipp et al., 1987; Tranquilly et al.,* 1987; *Richardson and Reames, 1993],* and smooth rotation of the magnetic field [*Burlaga et al., 1981; Lepping et al.,* 1990]. Some authors *[Montgomery et al., 1974] also* report depressed electron temperatures in CME plasma but a recent study by *Richardson et al. [1997]* indicates that the electron temperature is often increased within ejects plasma, In addition, faster CMES are usually preceded by a shock. Often, researchers have concentrated on only a single characteristic and hence many aspects of CMES may have been overlooked. In particular, little work has been done to understand how CME flows return to the ambient quasi-stationary state. Until relatively recently we have been able to measure CME characteristics only in or near the ecliptic plane, but since the out of ecliptic passages of the Ulysses spacecraft data from high latitudes have also been available *[Gosling et al.,* 1994]. This report focuses only on in-ecliptic data obtained by ISEE-3 and we leave a similar analysis of high latitude data for a future study.

In this paper we first look at the characteristics of a typical CME, then define a set of parameters based on the distinction between quiescent and transient heliospheric flow, and then present and discuss the statistics of these parameters for a set of CMEs identified in data from the ISEE-3 spacecraft near 1 AU during the period 1978 to 1980. We are particularly interested in what the measurements can tell us about how the CME evolves and how the corona returns to its quiescent state after the CME release. A preliminary report of this work was presented by *Neugebauer and Goldstein [1997].*

A CME Example

Although there might not be such a thing as a typical CME, Figure 1 shows data characteristic of many of these events. The figure plots solar wind proton speed (V_p), density (N_p), and temperature (T_p), and magnetic field strength (B) during the period September 28 to October 4, 1978. The plasma data are from the NSSDC OMNI set, while the field data are from ISEE-3, which was at L 1 during this period. (The bottom two panels will be described later.) The data show a shock at about Day 271.8 and another at about Day 272.1, with consequent sharp increases in velocity, temperature, and magnetic field strength at each. Subsequently, all three of these quantities decayed to their pre-shock values or much lower.

The top panel illustrates the period during which a CME passage was identified during this period by the criterion of: "C", a magnetic cloud [*Zhang and Burlaga, 1988]; "G",* bi-directional suprathermal electron streaming *[Gosling et al., 1987];* "M" [*Marsden et al., 1987]* and "R' *[Richardson and Reames, 1993],* hi-directional energetic ion streaming. The basic solar wind parameters do not show any obvious clues to what is happening in the CME, so we have tried investigating parametric relationships between these quantities to

distinguish quasistationary (QS) from transient (TR) solar wind flow. We have used the following relationships [*Neugebauer*, 1992]:

1) $T_p \propto$ VP, but weaker in TR, with T_p generally lower than in QS for a given VP;

2) B (TR) > B (QS), and β (TR) < β (QS);

3) N_α / N_p (HAE) > N_α / N_p (QS),

where the last relation is by definition for helium abundance enhancements (HAEs). From these relations we have defined a set of parameters which often exceed unity in transient flow:

1)11 = $(500V_p - 1.75 \times 10^5)/T_p$;

2)12 = 1 + log $(0.5/\beta)$;

3) $I_3 = (N_\alpha / N_p)/0.08$.

The β used in I_2 represents the total plasma and includes electrons, protons, and alpha particles. Each of these definitions is somewhat arbitrary, but appears to capture the difference between QS and TR flow most of the time. For example, the definition of I_1 is similar to that used by *Gosling et al. [1973], Neugebauer et al. [1997],* and *Richardson and Cane (1995,* for VP> 500 kms^{-1}). We point out, however, that our definition of I_1 is not a good identifier at low speeds, and therefore the results are somewhat biased toward high speed solar wind. See *Neugebauer et al.*, 1997 for further discussion of this point.

The usefulness of I_1 is largely a result of the expansion of the plasma cloud as it propagates away from the sun. Another way to see this effect is to look at the thermal Mach number. *(See* also *Neugebauer and Alexander [1991].)* Recently, *Farrugia et al. [1997] analyzed* the event of Fig. 1 and argued that the effect of expansion was a result of the presence of a magnetic cloud; we shall return to this issue later. Similarly, the significance of I_2 for

characterizing transient flow is the result of the relative changes in magnetic field (increase) and plasma temperature (decrease).

In Figure 2, the data for the period 1978 Day 271-277 are replotted using the above three parameters. The top panel again shows the previously reported CME intervals, and the bottom two panels give the elevation and azimuth angles, respectively, of the magnetic field direction. The interval over which index $I_1 > 1$ begins slightly earlier than the beginning of any of the C, G, M, R identifiers of hi-directional streaming or magnetic cloud, and extends more than 12 hours past the end of the longest ("R") period. Likewise, the other two indices begin earlier than and extend later than the C, G, M, R criteria for CME flow (although I_3 dips below unity during a large portion of the CME). The plot of magnetic field elevation (Θ) shows a smooth rotation of the field from south to north, in agreement with the previous identification of a magnetic cloud structure ("C").

In similar fashion, reference to the two bottom panels of Fig. 1 shows evidence of characteristics broader in time than the traditional. These two panels plot the flux of protons of energy> 60 MeV (from the NSSDC OMNI data set) and ground based neutron flux at the Deep River station [Solar-Geophysical data comprehensive reports, Number 416, Part II, April 1979]. Both of these show the effects of the CME ejecta/magnetic field blocking or deflecting cosmic rays away from the respective sensors. *Cane et al.* [1997] have recently discussed the association between the depression of> 60 MeV particle fluxes measured at Helios 1 and 2 and plasma signatures of ejects such as the depression of proton temperature. (See also *Cane et al.*, 1996)

Statistics

Several authors have published or compiled lists of CMES based on their favorite criteria, We have merged three sets based on ISEE-3 measurements [*Marsden et al.*, 1987, *Gosling*

et al., 1987, and *Richardson and Reames, 1993]* into a single list. Some events appear in all three, some in two and some in only one, showing the possible vagaries of the various criteria used to identify the CMEs. Table 1 shows a portion of the beginning of our merged, time-ordered list, illustrating this effect. The columns give the start year, day, and hour, the same for the end of the event, and a letter identifying the source. M is from the list of *Mars&net al.* [1987], G from *Gosling et al. [1987],* and R from *Richardson and Reames [1993].* The vertical heavy bars show how the different authors have identified different start and/or stop times for what is apparently the same event. To avoid counting more than once in our statistical study what is most likely the same event, we culled the list and retained only the earliest start time and the latest stop time of duplicate entries. So, for example, for the three entries for day 2721978 (marked by the rectangular box in Table 1) we use 0915 day 272 as the start and 0400 of day 273 as the end of the event. However, where only a short gap occurs between events in the list it is not always clear what is part of the previous event and what is a new event.

We calculated 1 hr averaged values of the indices I_1, I_2, and I_3 for the entire period for which both plasma and magnetic field data are available from ISEE-3 (August 1987 to February 1980). From the results we selected those periods for which index I_1 gave the strongest indication of transient flow, yielding 29 events. These are listed in Table 2. The start and stop times are from the merged list, and the letter designations for each event is as in Table 1. Multiple letters indicate the identification of the event by more than one technique. A superposed epoch analysis was then performed on these events, using various zero epoch times.

Figure *3,* one such result, is a histogram of the frequency of occurrence of hi-directional streaming of electrons or ions using the start of such detection (Table 2) as the zero epoch. The ordinate is the fraction of each hour in which the event occurs. For this ensemble the

average duration of CMES defined by hi-directional flow is thus 12 hrs. By definition, for this figure, there are no occurrences prior to the zero epoch.

Figure 4 (a, b, c) shows histograms for the three indices 1_1,12, and I_3, respectively, again using the hi-directional streaming start time (Table 2) as the zero of the epoch, In each case the ordinate gives the average fraction of each hour for which the index exceeds unity for the ensemble. The heavy horizontal line in each histogram is the average hourly fraction for which the index exceeded unity, calculated over the whole data set (approximately 11700 hourly intervals from August, 1987 to February, 1980), and which we take to represent the random probability of the index being >1. As in the case of the example in Fig. 2, we see that the indices show transient flow beginning earlier than the start of a CME as defined by the hi-directional streaming indicators G, M, and R about 10 to 30% of the time, as well as lasting longer than the flow intervals shown in Fig. 3.

An example of another way to see the relation between the start of hi-directional streaming and our indices is shown in Figure 5. This figure is a histogram of the frequency of occurrence of hi-directional streaming, but using $I_1>1$ as zero epoch, (The zero for the epoch was determined by the time within $\pm$ 24 hrs of the start of each event in Table 2 for which $I_1 > 1$ for most of the hour.) This shows that the hi-directional streaming doesn't generally start until several hours after the start of a CME if I_1 is used as indicator of the start.

Discussion and summary

The detection of bidirectionally streaming electrons or ions has been one of the more useful techniques for identifying passage of a CME across a spacecraft. These phenomena must be tied to the magnetic field topology at the CME, as discussed by several authors [e.g., Gosling, 1996]. Many of these authors have shown cartoons in an attempt to understand

the configuration of CMES, especially the relation between the shock (if present), magnetic field, and plasma within the CME. The results of our analysis, particularly shown in Figure 4, clearly indicate that the transient plasma making up the main body of the CME is not a well defined, nicely contained "parcel". This is probably a result of the expansion of the gas cloud as it travels away from the sun, as well as erosion of the nose of the CME by reconnection with the IMF as it travels through the interplanetary medium.

In this regard, we return to the issue of plasma expansion around magnetic clouds discussed by *Farrugia et al. [1997]*. We note that of the 29 events in our subset only 4 are included in previously published lists [*Zhang and Burlaga, 1988* and *Lepping et al.,* 1990] of magnetic clouds for the time period we have considered and an additional 4 of our events have likely magnetic clouds embedded. Hence the statistics shown by Fig. 4 indicate that the characteristics of an expanding plasma for a CME are not restricted to the case of embedded magnetic clouds. The expansion occurs independent of the magnetic configuration.

We have examined the plasma and field data for each of the events in our subset and conclude that a shock clearly precedes 23 of these 29 events. The mean time between the leading shock and start of these CMES (based on hi-directional streaming) is about 17 hours. Figure 4 shows that the transient plasma occasionally extends up to and through the shock, so there is not a distinct gap between what might be considered a driver gas and the shock itself. A specific example of this can be seen in Figure 6, which is a plot of solar wind plasma temperature, T_p (left axis) and index I_1 (right axis) for the period of days 315 through 318 of 1978. (This corresponds to the fifth event listed in Table 2.) The temperature (as well as density and velocity, not plotted here) shows a shock occurring at the start of day 316, whereas the index I_1 is >1 for several hours - half a day earlier. Such an appearance of transient plasma prior to the shock is an indication, as suggested by

previous authors [*Gosling and Riley, 1996]* that the transient gas parcel is not actually driving the shock but is just part of the whole eruptive process that initiated the CME.

The bidirectional streaming of ions or electrons is usually taken to indicate magnetic field lines with both ends connected back to the sun or in a completely closed configuration, In the latter case, the CME plasma would be a completely enclosed plasmoid and it would be expected that the plasma properties would recover to typical, quiescent solar wind values after the hi-directional flow ceased. But our results (cf. Figures 2,4, and 5) show that the flow remains transient for at least one or two days after the end of the BDS. This must mean that the field lines have either reconnected to the IMF or never formed a closed configuration in the first place. This is in agreement with recent discussions by *Gosling [1996]* and *Neugebauer et al.* [1997].

Acknowledgments

We acknowledge with thanks the NSSDC for use of OMNI data, Ed Smith for ISEE-3 magnetometer data [*Frandsen et al.*, 1978], and Jack Gosling for ISEE-3 plasma data [*Bame, et al.*, 1978]. We also thank Ian Richardson for some helpful comments about the >60 MeV proton fluxes, and Ian Richardson and Don Reames for an electronic version of their list of energetic ion events. This research was performed at the Jet Propulsion Laboratory under a contract between the California Institute of Technology and the National Aeronautics and Space Administration.

References

Bame, S. J. et al., ISEE-C solar wind plasma experiment, *IEEE Trans. Geosci. Electron., GE-16,* 160, *1978.*

Bame, S. J., Bidirectional streaming of solar wind electrons >80 eV: ISEE evidence for a closed-field structure within the driver gas of an interplanetary shock, *Geophys. Res. Lett., 8,* 173, 1981.

Borini, G. et al., Helium abundance enhancements in the solar wind, *J. Geophys. Res.,* 87, 7370, 1982.

Burlaga, L. E., E. Sittler, F. Mariani, and R. Schwenn, Magnetic loop behind an interplanetary shock: Voyager, Helios, and IMP 8 observations, *J. Geophys. Res., 86, 6673, 1981.*

Cane, H. V., I. G. Richardson, and T. T. von Rosenvinge, Cosmic ray decreases: 1964-1994, *J. Geophys. Res., 101,* 21561-21572, 1996,

Cane, H. V., 1. G. Richardson, and G. Wibberenz, Helios 1 and 2 observations of particle decreases, ejects, and magnetic clouds, *J. Geophys. Res., 102,7075-7086, 1997.*

Farrugia, C. J., N. V. Erkaev, H. K. Biernat, L, F. Burlaga, R. P. Lepping, and V. A. Osherovich, Possible plasma depletion layer ahead of an interplanetary ejects, *J. Geophys. Res., 102, 7087-7093, 1997.*

Frandsen, A. M. A. et al., The ISEE-C vector helium magnetometer, *IEEE Trans. Geosci. Electron., GE-16, 195, 1978.*

Gosling, J. T., Magnetic topologies of coronal mass ejection events: Effects of 3-dimensional reconnection, in *Solar Wind Eight,* edited by D. Winterhalter, J. T. Gosling, S. R. Habbal, W. S, Kurth, and M, Neugebauer, pp. 438-441, American Institute of Physics, Woodbury, New York, 1996.

Gosling, J. T., V. Pizzo, and S. J. Bame, Anomalously low proton temperatures in the solar wind following interplanetary shock waves - Evidence for magnetic bottles?, *J. Geophys. Res.,* 78, 2001-2008, 1973.

Gosling, J. T., D. N. Baker, S. J. Bame, W. C. Feldman, and R. D. Zwickl, Bidirectional solar wind electron heat flux events, *J. Geophys. Res.,* 92, 8519-8535, 1987.

Gosling, J. T. et al., The speeds of coronal mass ejections in the solar wind at mid heliographic latitudes: Ulysses, *Geophys. Res. Lett., 21,* 1109-1112, 1994.

Gosling, J. T., and P. Riley, The acceleration of slow coronal mass ejections in the high speed solar wind, *Geophys. Res. Lett.,* 23, 2867-2870, 1996.

Hirshberg, J. et al., Solar flares and solar wind helium enrichments: July 1965-July 1967, *Sol. Phys., 23, 467, 1972.*

Kutchko, F. J., P. R. Briggs, and T. P. Armstrong, The hi-directional particle event of October 12, 1977, possibly associated with a magnetic loop, *J. Geophys. Res.,* 87, 1419, 1982.

Lepping, R. P., J. A. Jones, and L. F. Burlaga, Magnetic field structure of interplanetary clouds at 1 AU, *J. Geophys. Res.,* 95, 11957-11965, 1990.

Marsden, R. G., T. R. Sanderson, C. Tranquilly, K.-P. Wenzel, and E, J. Smith, ISEE 3 observations of low-energy proton bidirectional events and their relation to isolated interplanetary magnetic structures, *J. Geophys. Res.,* 92, 11009-11019, 1987.

Montgomery, M. D., J. R. Asbridge, S. J. Bame, and W. C. Feldman, Solar wind electron temperature depressions following some interplanetary shock waves: Evidence for magnetic merging?, *J. Geophys. Res.,* 79, 3103, 1974.

Neugebauer, M. and C. J. Alexander, Shuffling footpoints and magnetohydrodynamic discontinuities in the solar wind, *J. Geophys. Res.,* 96,9409, 1991.

Neugebauer, M., Knowledge of coronal heating and solar-wind acceleration obtained from observations of the solar wind near 1 AU, in *Solar Wind Seven,* Proceedings of the 3rd COSPAR Colloquim, Goslar, Germany, 16-20 September 1991, edited by E. Marsch and R. Schwenn, pp 69-78, 1992.

Neugebauer, M, and R. Goldstein, Particle and fields signatures of coronal mass ejections in the solar wind, in *Geophysical Monograph: Coronal Mass Ejections: Causes and Consequences,* edited by N. Crooker, J. Joselyn and J. Feynman, in press, Amer. Geophys. Un., Washington, DC, 1997.

Neugebauer, M., R. Goldstein, and B. E. Goldstein, Features observed in the trailing regions of interplanetary clouds from fast coronal mass ejections, *J. Geophys. Res.,* accepted, 1997.

Palmer, I. D., F. R. Allure, and S. Singer, Bidirectional anisotropies in solar cosmic ray events: evidence for a magnetic bottle, *J. Geophys. Res.,* 83, 75, 1978.

Pilipp, et al. Characteristics of electron velocity distribution functions in the solar wind derived from the Helios plasma experiment, *J. Geophys. Res.*, 92, 1075, 1987.
Richardson, I. G. and H. V. Cane, Regions of abnormally low proton temperature in the solar wind (1965- 199 1) and their association with ejects, *J. Geophys. Res., 100*, 23397, 1995.
Richardson, 1. G. and D. V. Reames, Bidirectional ~1 MeV/amu ion intervals in 1973-1991 observed by the Goddard Space Flight Center instruments on IMP 8 and ISEE 3/ICE, *Astrophys. J. Suppl. Ser., 85, 411*, 1993.
Richardson, I. G., C. J. Farrugia, and H. V. Cane, A statistical study of the behavior of the electron temperature in ejects, *J. Geophys. Res.*, 102,4691-4699, 1997.
Sanderson, T. R. et al., Correlated particle and magnetic field observations of a large-scale magnetic loop structure behind an interplanetary shock, *Geophys. Res. Lett., 10,916*, 1983.
Sarris, E. T. and S. M. Krimigis, Evidence for magnetic loops beyond 1 AU, *Geophys. Res. Left.*, 9, 167, 1982.
Tranquilly, C. et al., Properties of a large-scale interplanetary loop structure as deduced from low-energy proton anisotropy and magnetic field measurements, *J. Geophys. Res.*, 92, 6, 1987.
Zhang, G. and L. F. Burlaga, Magnetic clouds, geometric disturbances, and cosmic ray decreases, *J. Geophys. Res.*, 93,2511-2518, 1988.

Tables

1. Sample of merged CME list.

2. List of selected strong CME events.

Figure Captions

Figure 1. The solar wind proton speed, proton density, proton temperature, magnetic field strength, flux of protons with energy> 60 MeV, and relative neutron flux at the Deep River monitor station are shown for the period day 271 through day 277 of 1978. The top panel shows the periods during which a CME passage was identified by various authors; see the text for explanation of the letter symbols.

Figure 2. The indices (see text) I_1, I_2, I_3, and magnetic field elevation and azimuth angles shown for the period day 271 through day 277 of 1978.

Figure 3. Superposed epoch analysis histogram for our selected list of events showing the fraction of each hour in which an event occurs, using the start of the events listed in Table 2 as the zero epoch. The time period is from 24 hrs before to 72 hrs after the zero epoch.

Figure 4. Superposed epoch analysis histograms for the indices I_1, I_2, and I_3 (a, b, c, respectively). In each case the fraction of the hour in which the index exceeds unity is shown for the period from 24 hrs before to 72 hrs after the zero epoch, and the solid horizontal line is the random fraction for the entire data set. The starts of the events listed in Table 2 were used for the zero epoch.

Figure 5. Superposed epoch analysis histogram of Bi-directional streaming using the time within +/- 24 hrs of the start of the events in Table 2 for which $I_1 > 1$ for most of the hour was used as zero epoch. The ordinate gives the fraction of each hour for which bi-directional streaming occurred.

Figure 6. Plasma temperature, T_p, (left axis) and index I_1 (right axis) for days 315 through 318 of 1978. A shock occurs at the start of day 316, whereas I_1 exceeds unity for several hours earlier than this, indicating the presence of transient flow ahead of the shock.

Table 1. Sample of merged CME list (all in 1978)

DOY start	Hrmin start	DOY end	Hrmin end	Source
239	1350	239	1410	G
239	2000	239	2400	G
239	2000	240	200	M
253	200	253	1800	G
253	900	253	1400	R
263	100	263	1305	G
269	1400	269	2110	G
272	915	272	2245	R
272	1150	272	2315	G
272	1200	273	400	M
273	600	273	1130	R
273	1545	273	2145	R
277	600	278	730	R
280	1230	280	1800	R
280	2145	281	745	R
281	1430	282	0	R
284	2145	285		R
294	715	294	1%0	R
302	2200	303	700	M
302	2240	303	30	G
303	1540	304	800	G

Table 2. List of selected CME events.

Year	DOY start	Hrmin start	DOY end	Hrmin end	Source
78	253	200	253	1800	G, K
78	269	1400	269	2110	G
78	272	915	273	400	R, G, M
78	302	2200	303	700	M, G
78	316	1430	317	1100	G, M
78	328	2010	329	910	G
78	349	2315	350	700	R, M
78	359	1715	359	1900	G
79	2	2300	3	2230	R
79	6	345	6	2145	R
79	7	0	8	1000	M, R, G
79	43	1200	45	2015	M, R
79	54	900	54	1900	R, M, G
79	67	1730	68	100	R
79	68	1800	69	1030	R, G
79	70	1400	71	1200	R
79	80	2015	81	515	R
79	81	1630	81	1715	G
79	88	800	88	1430	G
79	89	245	89	1400	R
79	93	0	93	915	G, R
79	96	145	96	1500	R
79	115	1110	115	2330	G
79	162	1315	162	1815	R
79	185	2000	186	215	R
79	224	845	224	1845	R
79	235	1330	235	1915	R
80	13	1700	14	130	R
80	45	1445	46	45	R

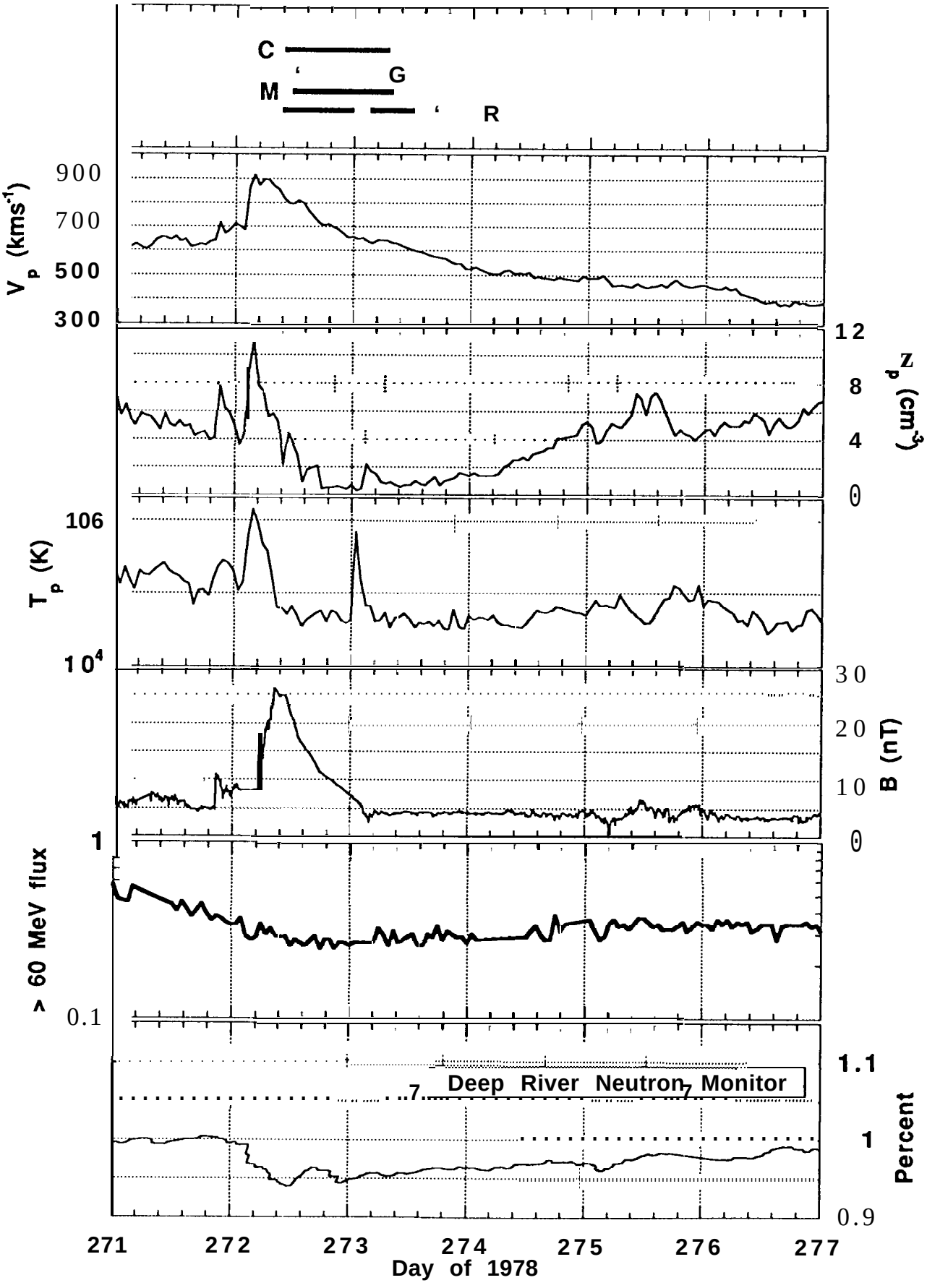
C
M
G
R
900
700
500
300
V_p (kms^{-1})
12
8
4
0
N_p (cm^{-3})
106
10^4
T_p (K)
30
20
10
0
B (nT)
1
0.1
> 60 MeV flux
Deep River Neutron Monitor
1.1
1
0.9
Percent
271
272
273
274
275
276
277
Day of 1978

Figure 1

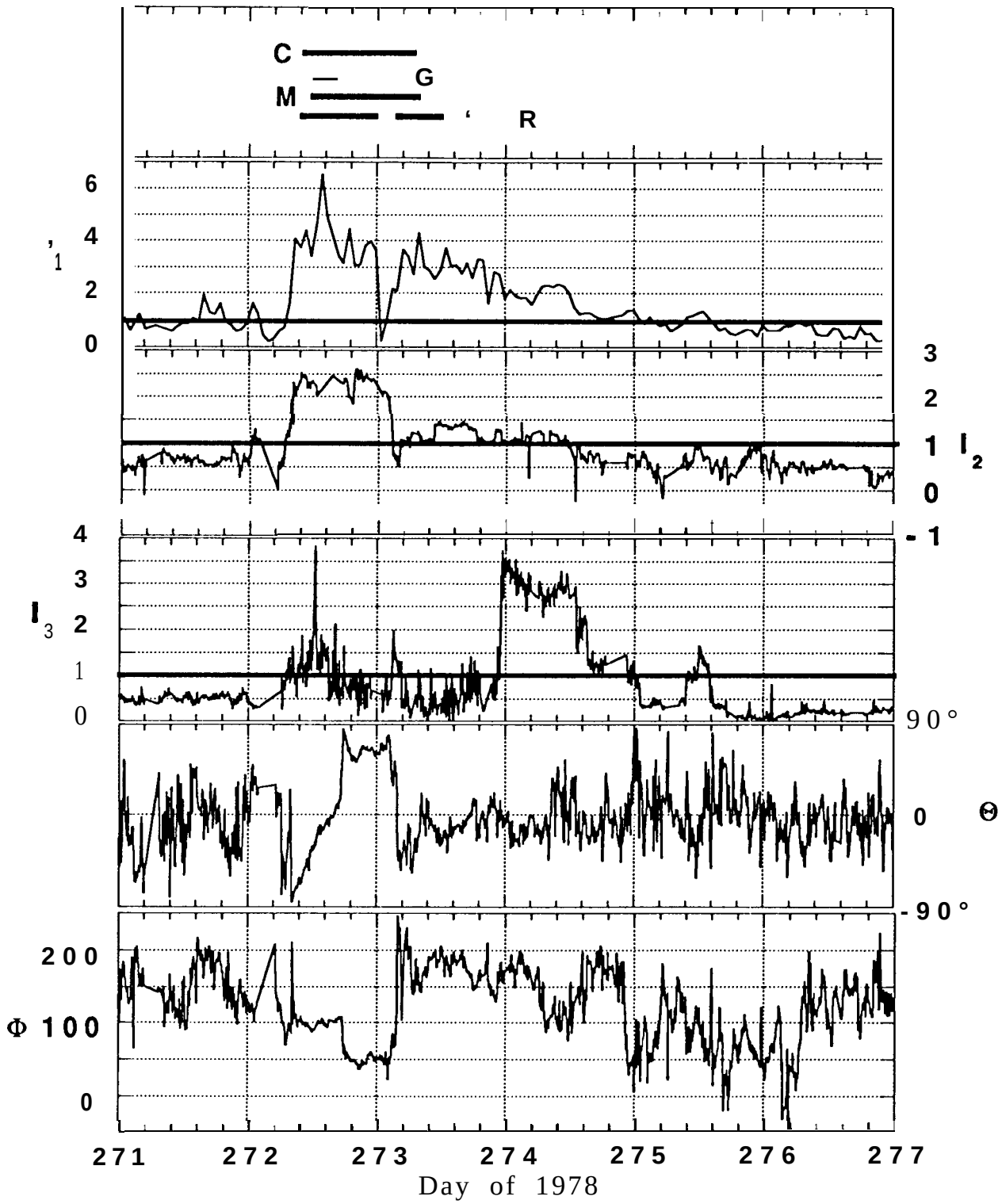
C
G
M
R
I1
6
4
2
0
3
2
1
I2
0
-1
I3
4
3
2
1
0
90°
0
Θ
-90°
Φ
200
100
0
271
272
273
274
275
276
277
Day of 1978

Figure 2

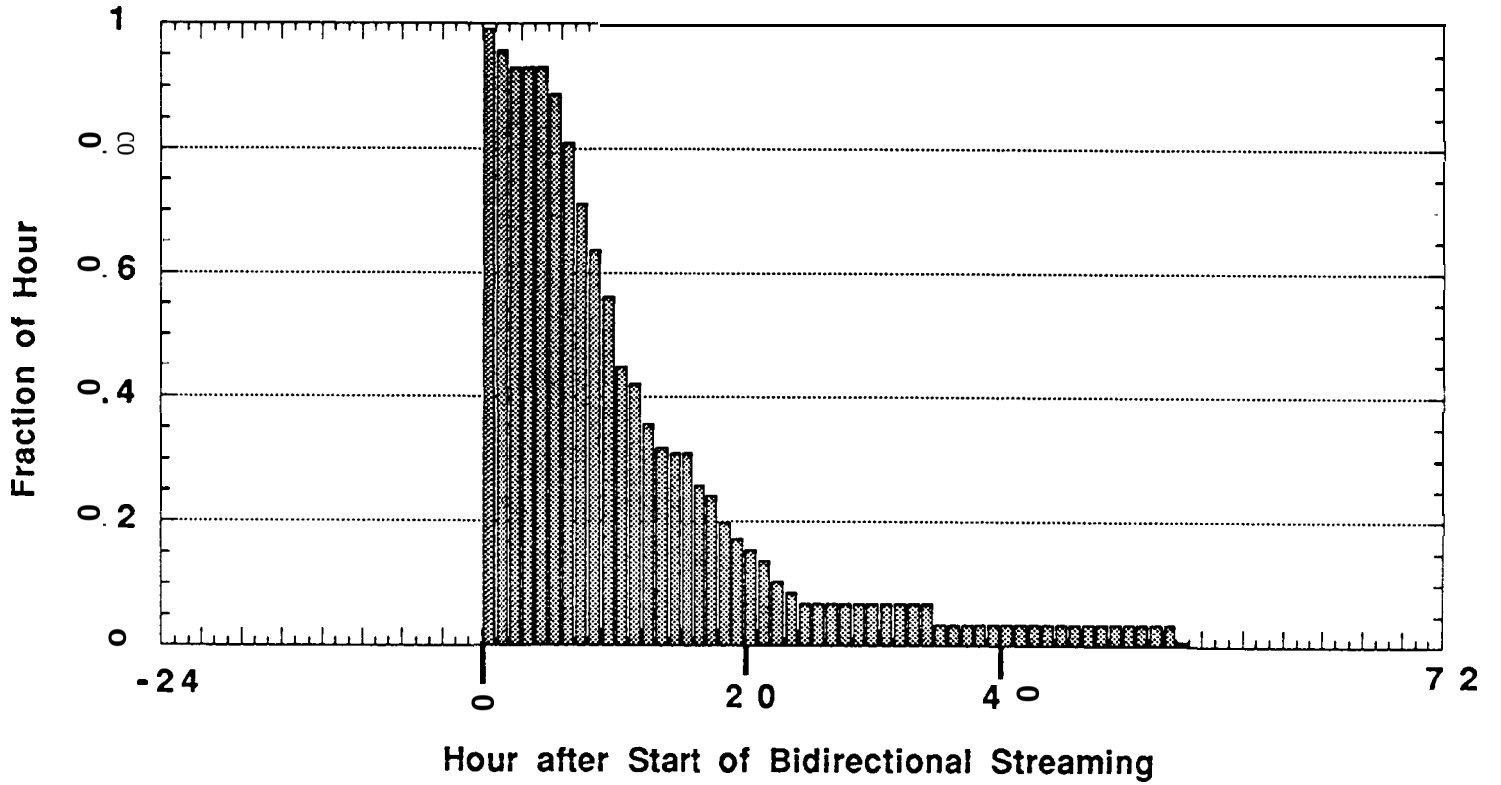
1
0.8
0.6
0.4
0.2
0
Fraction of Hour
-24
0
20
40
72
Hour after Start of Bidirectional Streaming

Figure 3

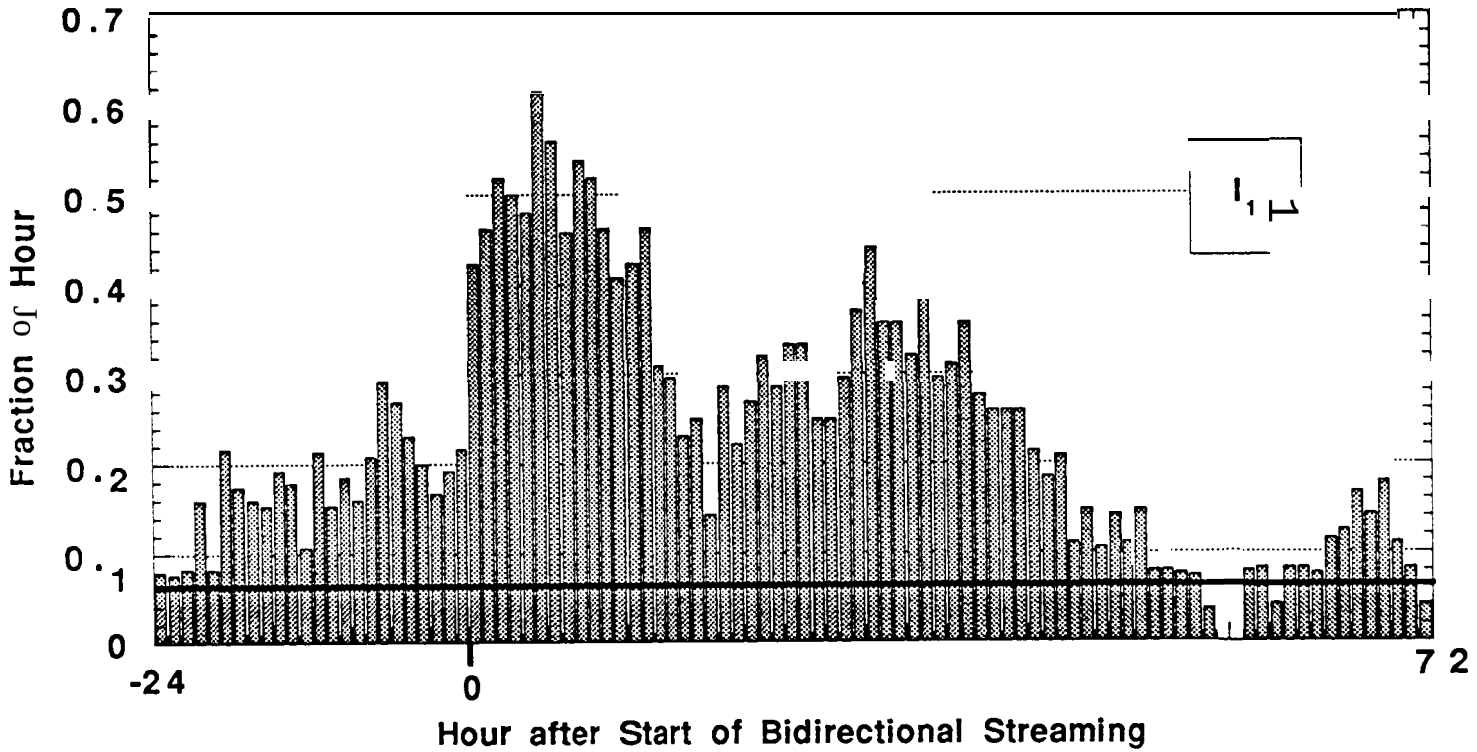
0.7
0.6
0.5
0.4
0.3
0.2
0.1
0
Fraction of Hour
-24
0
72
Hour after Start of Bidirectional Streaming

Figure 4a

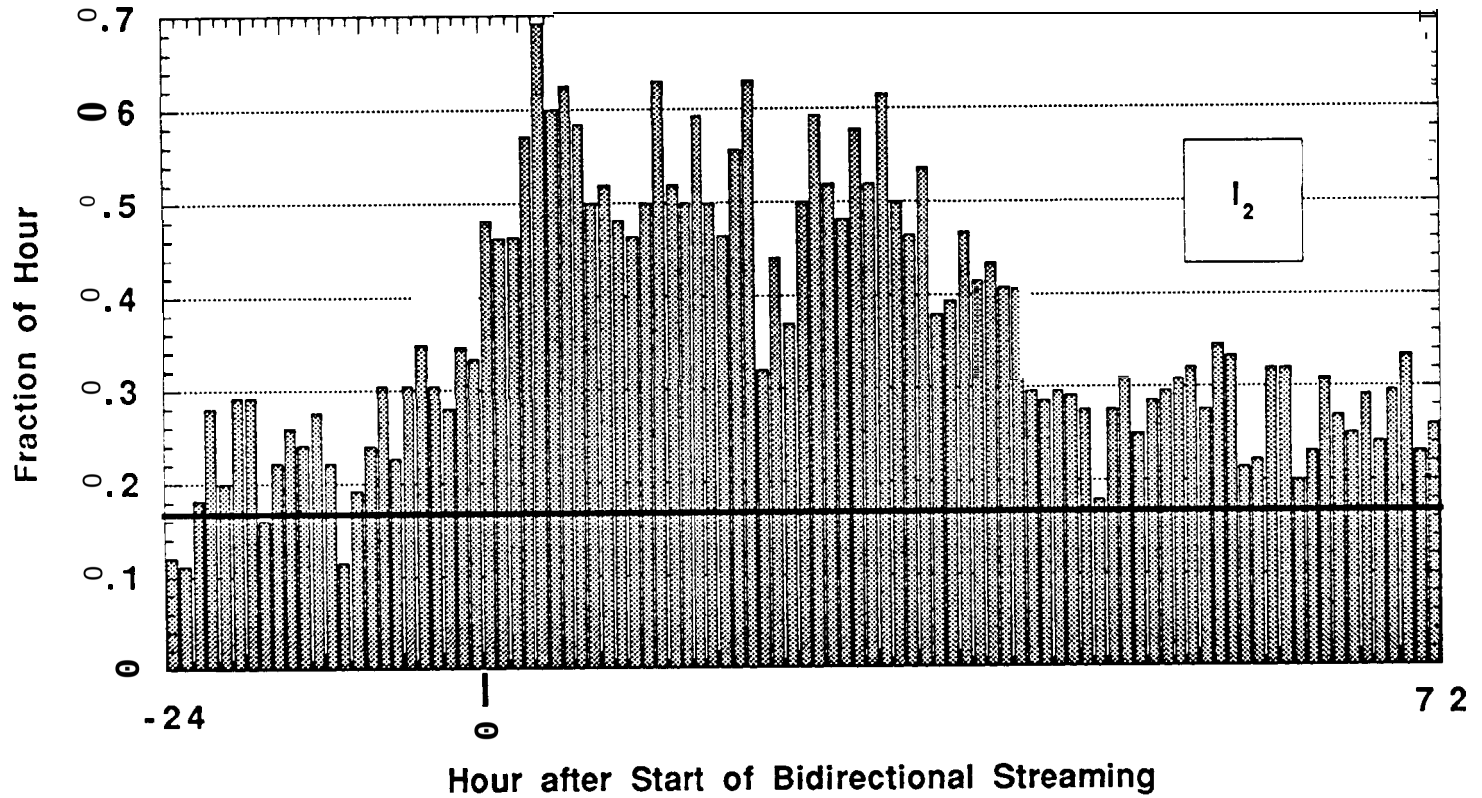
Fraction of Hour
0.7
0.6
0.5
0.4
0.3
0.2
0.1
0
I_2
-24
0
72
Hour after Start of Bidirectional Streaming

Figure 4b

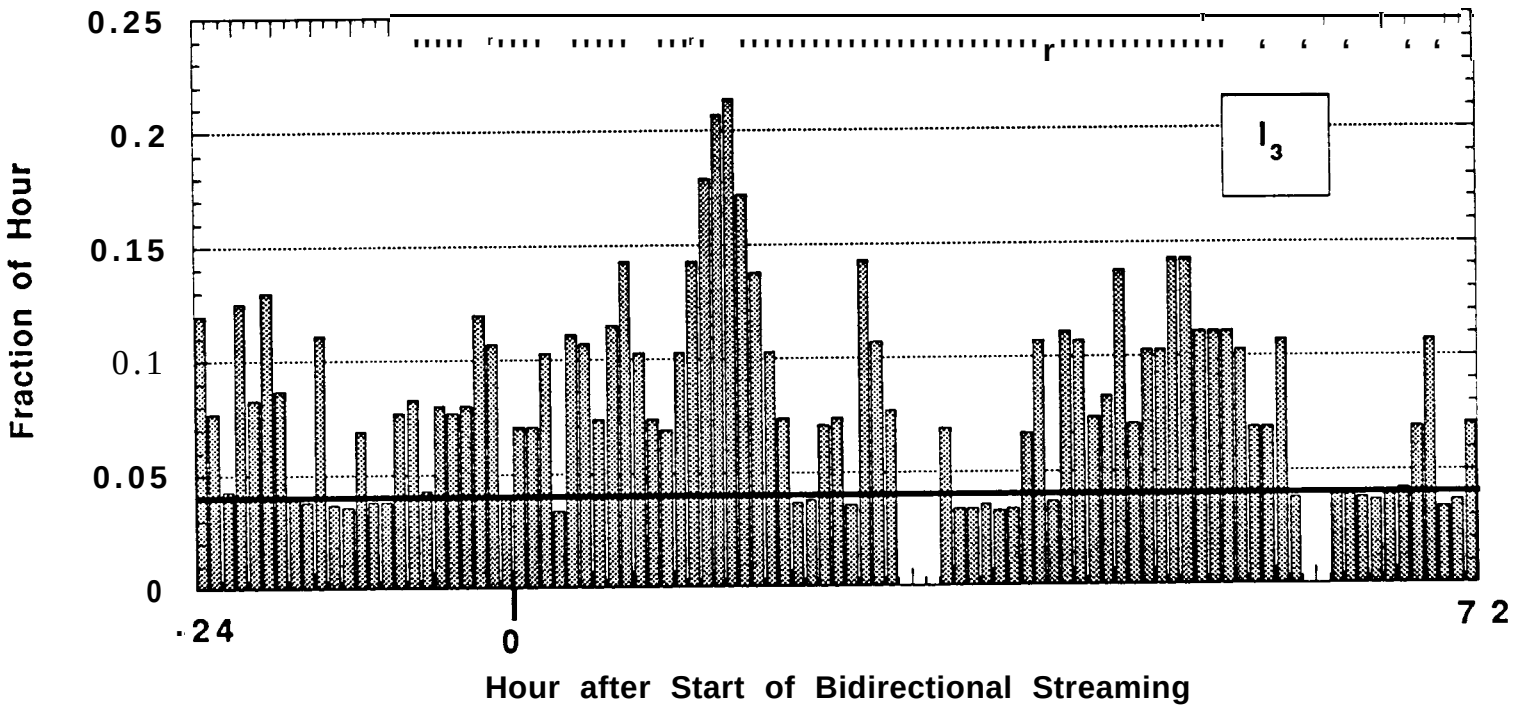
0.25
0.2
0.15
0.1
0.05
0
Fraction of Hour
I3
-24
0
72
Hour after Start of Bidirectional Streaming

Figure 4c

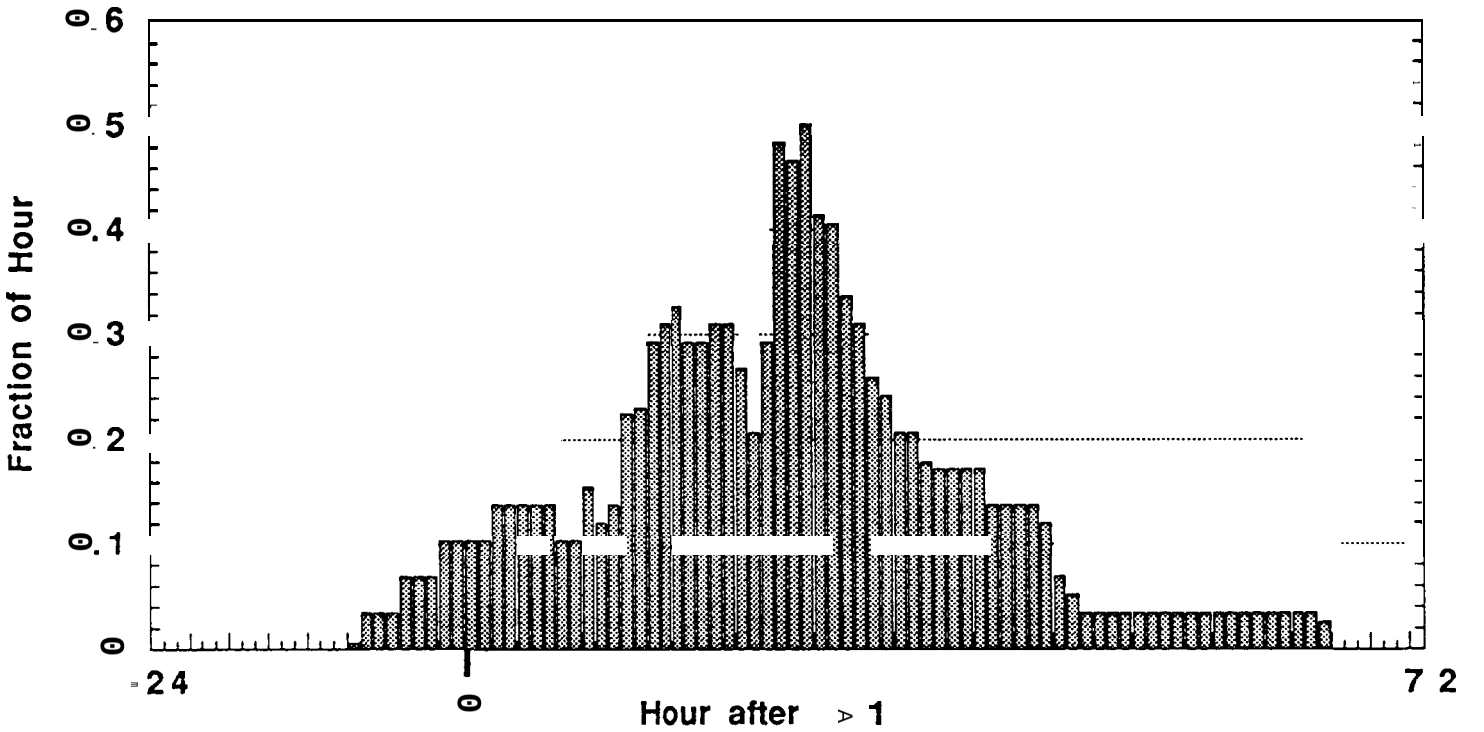

Figure 5

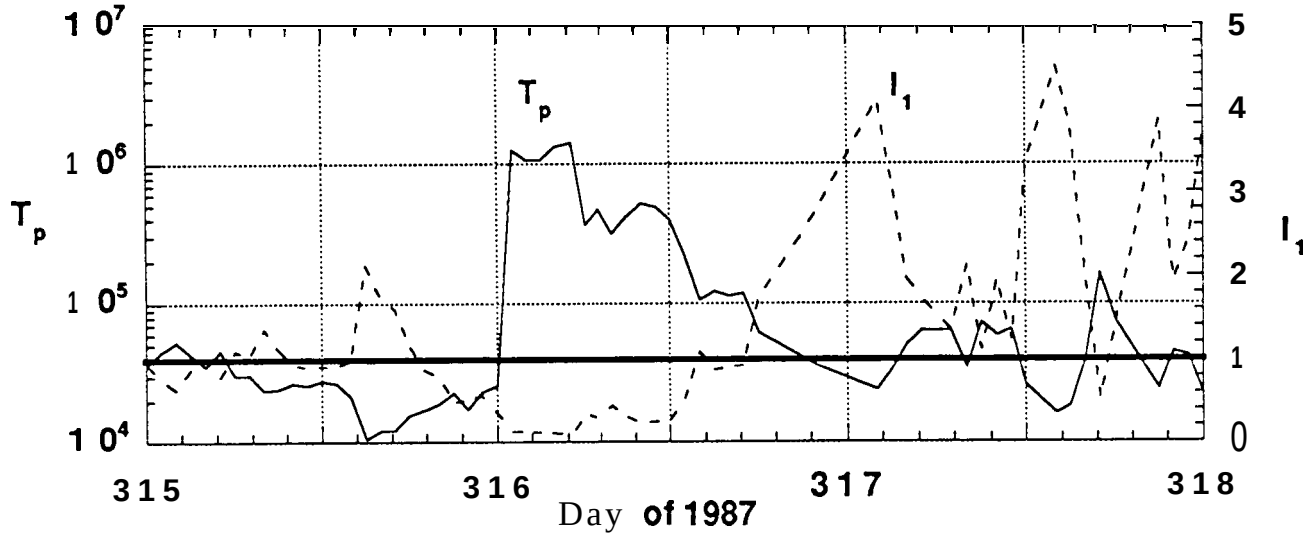

Figure 6